PAPER

A Cause of Momentary Level Shifts Appearing in Broadcast Satellite Signals

Ryouichi NISHIMURA[†a)], ***Senior Member***, **Byeongpyo JEONG**[†], **Hajime SUSUKITA**[†], ***Nonmembers***, **Takashi TAKAHASHI**[†], ***Member***, ***and*** **Kenichi TAKIZAWA**[†], ***Nonmember***

SUMMARY The degree of reception of BS signals is affected by various factors. After routinely recording it at two observation points at two locations, we found that momentary upward and downward level shifts occurred multiple times, mainly during daytime. These level shifts were observed at one location. No such signal was sensed at the other location. After producing an algorithm to extract such momemtary level shifts, their statistical properties were investigated. Careful analyses, including assessment of the signal polarity, amplitude, duration, hours, and comparison with actual flight schedules and route information implied that these level shifts are attributable to the interference of direct and reflected waves from aircraft flying at approximately tropopause altitude. This assumption is further validated through computer simulations of BS signal interference.

key words: *aircraft, bistatic radar, fresnel zone, IoT, remote sensing*

1. Introduction

Satellite broadcasting and communication services are available worldwide. They are especially useful for communications with distant islands and valleys among mountains, where communication using digital terrestrial broadcasting waves has difficulty because of the effects of obstacles and distance attenuation. The degree of broadcast satellite (BS) signal reception is affected by various factors such as precipitation from the atmosphere, ionosphere conditions or obstacles on the ground such as buildings and trees [1]–[3]. In general, these factors lead to temporally slow variation, for example, over durations longer than minutes, in the receiving signal level. Because the primary purpose of the satellite broadcasting and communication services is to deliver contents to audiences, one can use a booster to compensate for level attenuation. If regional attenuation trends are known, then influence by precipitation might be mitigated by strengthening the signal that is transmitted toward the region in advance according to a priori information related to the predicted level attenuation [4].

Actually, BS signals could be used for other purposes such as remote sensing. Nishimura et al. routinely recorded broadcast satellite signals of intermediate frequency to assess the possibility of BS signals for use in the early detection of sudden rainstorms [5]. Reportedly, estimating the amount of rain is not easy, but it is possible to predict the location and timing of rainfall. Therefore, if one can construct a sensor array by connecting a BS antenna on the roof of each house, the detection of abrupt heavy rains can be achieved with higher spatial resolutions. Kawamura et al. proposed a method for estimating water vapor using digital terrestrial broadcasting waves to improve the accuracy of numerical weather forecasts for severe weather phenomena such as localized heavy rainstorms in urban areas [6]. When using this method, water vapor near a ground surface is estimated based on the propagation delay of digital terrestrial broadcasting waves.

Nagahora et al. investigated the cause of level variation in the receiving signal of the ground broadcasting service through a model calculation [7]. The model specifically shows three waves: the direct wave, the reflection wave from the ground, and that from an airplane. The model calculations revealed that the fluctuation level exceeds 2 dB. In fact, it sometimes reaches more than 4 dB. Because the ground broadcasting service is considered, a transmitter is assumed to be on the ground for this study. In general, a bistatic radar system, where the transmitter and the receiver stand at opposite sides of each other to the target object, is more sensitive than a monostatic radar, where the transmitter and the receiver are both on the same side. Glaser presented a technique for predicting the bistatic radar cross section (RCS) of an arbitrarily shaped object [8]. Effects of aircraft were examined in this study, but because it was based on Babinet's principle [9], only its silhouette was considered. The scattered radiation is related only to the object's silhouette.

As in our early study [5], we continued to record BS signals. We recently found that remarkable level shifts often appear in the recorded data at certain observation points. Sophisticated error correction coding would be sufficient to keep the digital information unaltered from a viewpoint of broadcasting and communications. However, identifying the cause of the level shift is important if the signal is to be used for remote sensing. To do that, we first defined the algorithm for extracting such a level shift. Then we investigated the statistical properties of the level shift with respect to its variations, duration, and number of occurrences [10]. As described in this paper, we further advance our early study [10] by adding data of different seasons of the year and by performing computer simulations of actual BS radio frequency signals with a reflection model incorporating flying airplanes.

The remainder of this paper is structured as described

Manuscript received August 19, 2022.
Manuscript revised December 26, 2022.
Manuscript publicized February 24, 2023.

[†]The authors are with National Institute of Information and Communications Technology, Sendai-shi, 980-0812 Japan.
a) E-mail: ryou@nict.go.jp

DOI: 10.1587/transcom.2022EBP3135

hereinafter. Measurement systems and observation conditions are explained in Sect. 2. In Sect. 3, two possible reasons for the level shifts are presented. Through various statistical analyses of properties of the observed level shifts, a promising cause is identified in Sect. 4. Then Sect. 5 provides additional discussion. Conclusions and future research topics are presented in Sect. 6.

2. BS Signal Observation

2.1 Measurement Setup

We have been recording BS signals in the cities of Sendai and Kashima. Kashima is located approximately 300 km south of Sendai, in Japan. The setup of measurement systems on both sites is depicted in Fig. 1. The BS signal is recorded simultaneously with two systems indicated by (a) and (b) in Fig. 1 at Sendai. Both antennas are mounted on the roof of a four-story building. They are approximately 20 m apart from each other in horizontal distance. No remarkable obstacle exists in the direction of BS satellites around the antennas. The antenna used in system (b) had been initially installed in the building for general TV use. The signal is captured at an antenna wall jack in a room. According to the electrical system diagram of the building, a booster is inserted between the antenna and the wall jack. The measurement setup in Kashima is identical to that used in Sendai. Only setup (a) was used. The two systems are approximately 455 m distant from one another in Kashima. All observed signals are transmitted constantly to a storage server in Sendai using a wireless broadband communication service.

The output of the low noise block converter (LNB) of a BS antenna is fed to a software defined radio (SDR, bladeRF x40; Nuand), where a baseband signal is extracted from the input intermediate frequency (IF) signal using a specified center frequency and band-pass filter. The filter bandwidth was set to 28 MHz because of the limitation of the SDR, although that of BS signal is 34.5 MHz. The center frequency was set to 1049.48 MHz, which is the center frequency of BS-1 channel, as shown in Fig. 2 [11]. The block diagram of the signal processing applied to the output of the SDR is depicted in Fig. 3. The data source is the output of the SDR, which is the I-Q signal of the BS signals sampled at 40 MHz, 12 bit, and represented in a sequence of a pair of complex numbers. To calculate the level of received BS signal, the obtained signal is first converted into its squared amplitude. It is then processed with a low-pass filter followed by decimation twice to obtain the signal at a sampling rate of 10 Hz. After it is transformed into a decibel representation, it is recorded in a file that contains samples for a duration of 10 minutes. Before storing the data in a file, 120 is uniformly added to the level data to represent it in the specified units: dBμV. In addition, the amount of insertion loss by the power supply and the impedance converter are compensated. The spectrum analyzer shown in Fig. 1 was used to guarantee that

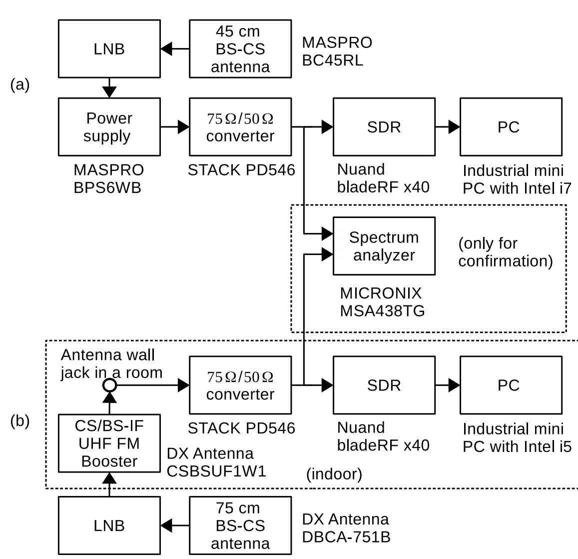

Fig. 1 System setup for recording the levels of the received BS signals.

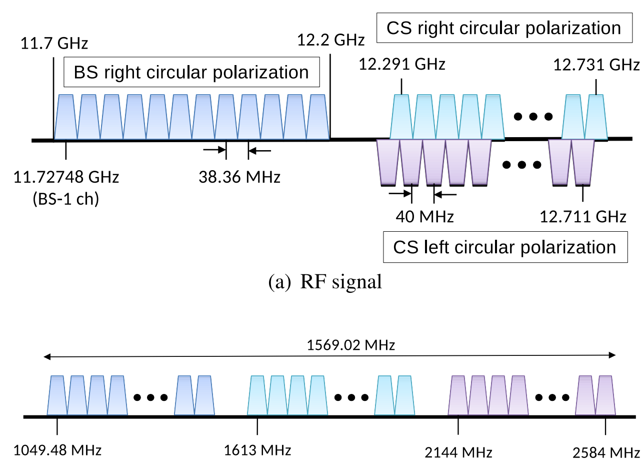

(a) RF signal

(b) IF signal

Fig. 2 Frequency assignment for broadcast satellites (BS) and communication satellites (CS), where 10.678 GHz and 10.127 GHz local transmission frequencies are assumed, respectively, for right and left circular polarization.

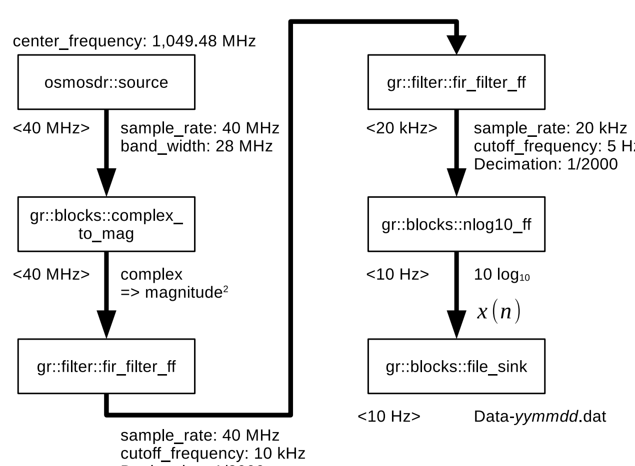

Fig. 3 Signal processing with GNU radio applied to the output of SDR before recording the level of BS signals.

Table 1 Summary of observation conditions.

Places	two positions each in Sendai and Kashima
	(38°15′07.3″N, 140°52′36.5″E) ⇒ Sendai (1)
	(38°15′07.0″N, 140°52′35.9″E) ⇒ Sendai (2)
	(35°57′22.5″N, 140°39′45.4″E) ⇒ Kashima (1)
	(35°57′20.1″N, 140°39′26.9″E) ⇒ Kashima (2)
Period	25 July, 2021 to 21 August, 2021
	7 November, 2021 to 4 December, 2021
Broadcast satellite	BSAT-3 at 110° East longitude
Direction of BS	(35.3°, 224.0°) at Sendai # (Elev., Azim.)
	(37.4°, 224.7°) at Kashima

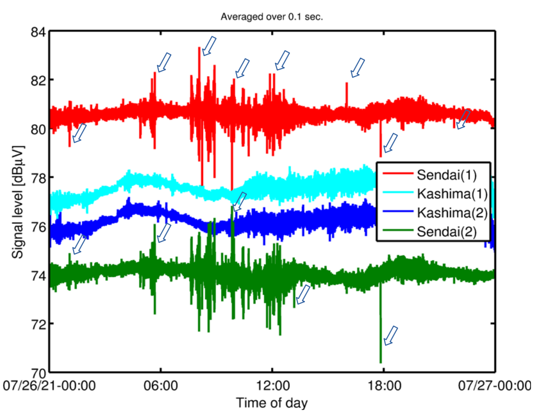

Fig. 4 Example of the observed BS signal level for one day. Some level shifts are indicated by arrows.

the numerical data obtained using this process are correct. Other measurement conditions are presented in Table 1.

2.2 Obtained Signal

The BS broadcasting service operated in Japan exploits either Trellis coded 8-ary phase shift keying (TC8PSK), quadratic phase shift keying (QPSK) or binary phase shift keying (BPSK) as an encoding method. The most appropriate method is selected among them, depending on the condition of propagation path to keep the quality of service higher than a certain level. Therefore, the level of receiving signal is fundamentally important independent from the broadcasting contents because only phase information is altered no matter what encoding method is selected. The received radio frequency (RF) signal is transformed to obtain the intermediate frequency (IF) signal. This encoding and decoding process inherently retain the signal level. Therefore, if one can assume system gains to be static, it is expected that the level of receiving BS signals directly reflects the transfer function of the propagation path.

Figure 4 presents an example of the recorded data for one day. As shown in this figure, it is evident that the data obtained at the observation points in Sendai include multiple distinct level shifts, which do not appear in those obtained in Kashima. Those level shifts appear in a manner that is similar in some respects and different in others between the measurement systems at Sendai. Possible reasons for these level shifts are discussed in the next section.

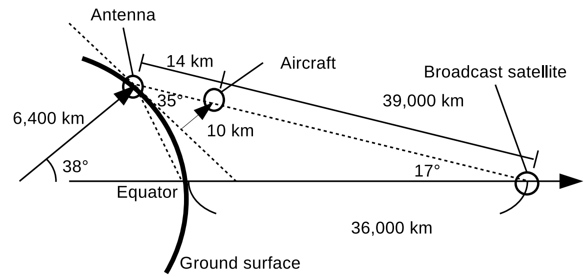

Fig. 5 Geometrical relation when receiving the BS signal at Sendai.

3. Possible Causes of Level Shifts

3.1 Shadowing

One reason of the level shifts might be the shadowing by some object passing across the propagation path of the BS signal between the broadcast satellite and the observation point. The first Fresnel zone is defined as the internal area of the ellipse determined by such a trajectory that the sum of the distances from two focal points is equivalent to the shortest length between them [12]. This area plays a prominent role in signal propagation. Conversely, the shadowed area by an object in the first Fresnel zone will determine how much the signal propagation is hindered. The radius of the first Fresnel zone is written as

$$\rho = \sqrt{\lambda \frac{d_1 d_2}{d_1 + d_2}}, \tag{1}$$

where λ stands for the wavelength, and where d_1 and d_2 respectively denote the distances from the shadowing object to the transmitter and the receiver.

Figure 5 presents an example of the topological relation between a geostationary satellite as a transmitter and an antenna on the earth as a receiver. A broadcast satellite is traveling along a geostationary orbit approximately 36,000 km above the equator. One of the actual observation points used for the experiment in this study is assumed as the observation point. Distances presented in this figure are approximations because the azimuth angle of the BS satellite is not exactly south. The radius of the first Fresnel zone can be derived using these distances as

$$\rho = \sqrt{0.0256 \cdot \frac{14 \cdot 10^3 \cdot 39 \cdot 10^6}{14 \cdot 10^3 + 39 \cdot 10^6}} \simeq 18.9, \tag{2}$$

where $\lambda = 25.6$ mm is assumed, considering the lowest radio frequency of BS signals, 11.7 GHz. Because the wavelength becomes shorter as the signal frequency increases, the first Fresnel zone provided by (2) is the widest for BS signals. The first Fresnel zone has only 18.9 m in radius, as calculated in (2). It is unlikely that airplanes flying in the altitude of the tropopause shadow the BS signal receiving at a certain point multiple times every day.

For later discussion, the time duration for which the level is affected by a flying airplane is estimated here. Boeing 767-300, which is one of the models actually used for domestic flights in Japan, is 54.9 m long, 47.6 m wide, and 15.9 m high. Its cruising speed is 880 km/h, according to the information provided in information for this aircraft [13]. Therefore, this aircraft might shadow the BS signal for a duration of 54.9/88000*3600 = 0.22 s when it passes perpendicularly across the propagation path of the BS signal.

3.2 Interference

Another possible factor of level shifts is interference between two or more electromagnetic waves. Hajkowicz reported in [14] that quasiperiodic scintillation events are present in the recorded signals of the VHF radio-satellite transmissions at a frequency of 150 MHz. In many cases, they are associated with ionospheric irregularities. However, some of them resulted from the interference of electromagnetic waves that are simultaneously transmitted within the bandwidth of the same receiving antenna. Such a situation might occur when signals from both a moving orbiting satellite and a geostationary satellite are received simultaneously. Another possibility is a stationary transmitter: a TV station. In any case, the resultant quasiperiodic scintillation events have a ringing structure and a duration of a few to some several seconds.

Current digital BS communication systems use much higher frequency than those used in the early study [14]. Therefore, the phenomena might change. Revision of the knowledge obtained in the past would be required. In this respect, we assume that an aircraft might be an object to generate an interference wave because it has a cylindrical body and because it can reflect radio waves in many directions. The effect is expected to persist for the same duration as that estimated for the shadowing effect in the previous section: 0.22 s. We prove this assumption in the following sections.

4. Statistical Analysis of Properties

4.1 Detection of Momentary Level Shifts

Figure 6 schematically explains how momentary level shifts are defined and extracted in this study. The received signal level $x(n)$ is first divided into consecutive segments of time length T, where n indicates the sampling time and its interval was set to 0.1 s as shown in Fig. 3 for the duration analysis in Sect. 4.3. Written with the m-th segment as S_m, candidates of positive level shift N_+ and negative level shift N_- are obtained by

$$\begin{cases} N_+ = \{n \mid x(n) \geq \mathrm{E}[x(n|n \in S_m)] + \alpha \cdot \sigma_m\}, \\ N_- = \{n \mid x(n) < \mathrm{E}[x(n|n \in S_m)] - \alpha \cdot \sigma_m\}, \end{cases} \tag{3}$$

where

$$\sigma_m = \sqrt{\sum_{n \in S_m} \{x(n) - \mathrm{E}[x(n)]\}^2} \tag{4}$$

and α is a parameter to control sensitivity.

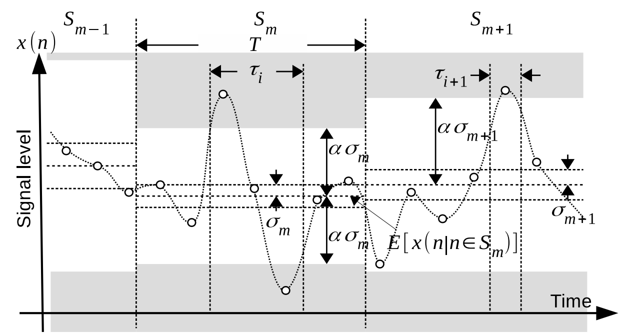

Fig. 6 Schematic explanation of the algorithm for extracting mometary level shifts.

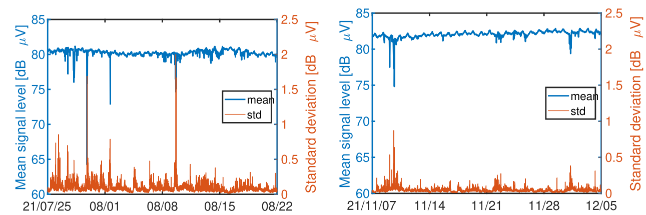

(a) Summer (b) Autumn

Fig. 7 Mean and standard deviation of the received BS signal level at Sendai (2) for every minute of data.

In addition to those obtained by (3), single points adjoining candidates having opposite polarity on each side are also regarded as candidates of momemtary level shift because they are presumably the transition points. This process can be formulated as the following. First define

$$\phi(n) \equiv \begin{cases} 1 & n \in N_+ \\ -1 & n \in N_- \\ 0 & \text{otherwise,} \end{cases} \tag{5}$$

and then extract a group

$$N_o = \{n \mid \phi(n-1) \cdot \phi(n+1) = -1\}. \tag{6}$$

Combining (3) and (6), candidates of momentary level shift are finally obtained by collecting their union as

$$N = N_+ \cup N_- \cup N_o. \tag{7}$$

Consecutive $n \in N$ is regarded as a single level shift.

Based on the momentary level shifts detected using the algorithm described above, statistical analysis of their properties was performed as described in the following subsections. Figure 7 shows the received BS signal level and its standard deviation for the whole measurement period presented in Table 1. It is likely to be raining when the standard deviation becomes large because of the rain attenuation. Detection accuracy of momentary level shift would become low for these time periods. However, we give no special treatment to them in the following statistical analyses. Table 2 presents the resultant figures and sections in which they are discussed.

Table 2 Statistical analyses and corresponding figures and sections.

Figure	Statistical property	Section
Fig. 8	polarity of level shift	4.2
Fig. 9	appearance for each hour	4.2
Fig. 10	duration of level shift	4.3
Fig. 11	amount of level shift	4.4

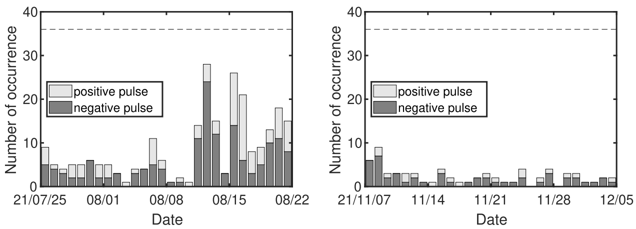

(a) Summer (b) Autumn

Fig. 8 Number of positive (light gray) and negative (dark gray) level shifts during the experiment. The dashed lines represent the number of flights bound for Tokyo from Sapporo [15].

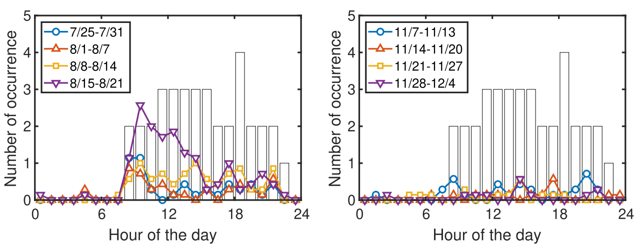

(a) Summer (b) Autumn

Fig. 9 Number of momentary level shift occurrences for every hour of the day, averaged over each week. Bars represent those obtained from the flight schedule bound for Tokyo from Sapporo [15].

4.2 Number of Occurrences

Statistical analysis is applied to the data obtained in Sendai, assuming $T = 1$ minute in Fig. 6 and $\alpha = 6$ in (3). Considering the speed of level change, these parameters are chosen so that the level disturbance, probably because of water vapor, can be eliminated. Figure 8(a) shows the mean and standard deviation of the level of the received BS signal for each analysis window, whereas Fig. 8(b) shows the number of momentary level shifts detected by the algorithm described in the previous section for each day over the whole period of experiment. The number of daily flights bound for Tokyo from Sapporo, as indicated by a dashed line in Figs. 8(a) and 8(b), is calculated according to the timetable presented at the Sapporo airport web site [15].

The data are further analyzed to obtain weekly statistics because not all flights are in service every day. The results are shown in Fig. 9, where those calculated from the flight schedule are presented as a bar plot. According to information obtained by flightradar24 [16], it is likely that flights bound for Tokyo from Sapporo passing the point near the propagation path of the BS signal receiving at Sendai 45 minutes after its departure. The bar plots are made from

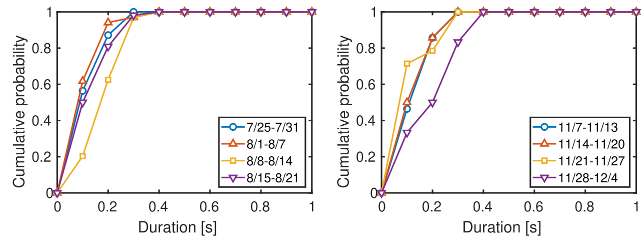

(a) Summer (b) Autumn

Fig. 10 Empirical cumulative distribution functions of the durations of level shifts.

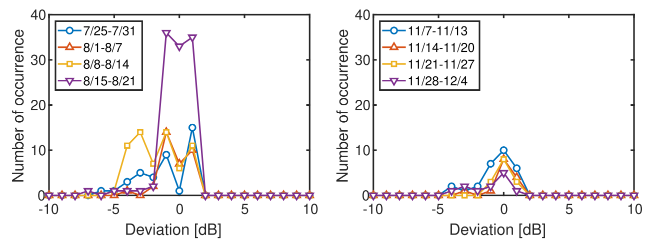

(a) Summer (b) Autumn

Fig. 11 Histogram of the amount of level shift.

the times obtained considering this flight time delay.

We also find other notable trends in these figures. Negative level shifts appear more likely than positive ones. There is good coincidence between the timing of flights and occurrence of momentary level shifts. Apparently, momentary level shifts appear more frequently during summer than during autumn.

4.3 Duration

The duration of level shift, τ in Fig. 6, is defined by the product of sampling period and the number of samples constituting the level shift. The level data are finally recorded at a sampling rate of 10 Hz, yielding resolution of 0.1 s. Figure 10 shows empirical cumulative distribution functions calculated for each week. As might be apparent from this figure, the duration of level shifts is, in most cases, shorter than 0.3 s, which is in good agreement with that estimated assuming an actual airplane, 0.22 s, as described in Sect. 3.1.

4.4 Level Variation

The level variation of the received BS signal is defined as

$$\Delta_x = \max_n [x(n) - \mathrm{E}[x(n|n \in S_m)]], \qquad n \in N, \qquad (8)$$

for each level shift. Figure 11 presents a histogram of level variation defined by (8). Both in summer and autumn, although positive level variation is less than 2 dB, the negative level variation spreads over −5 dB. Therefore, asymmetry exists with respect to zero. Because small level variation is essentially not detected as momentary level shift by the algorithm described in Sect. 4.1, it is not strange that the number of occurrences decreases in the proximity of the no

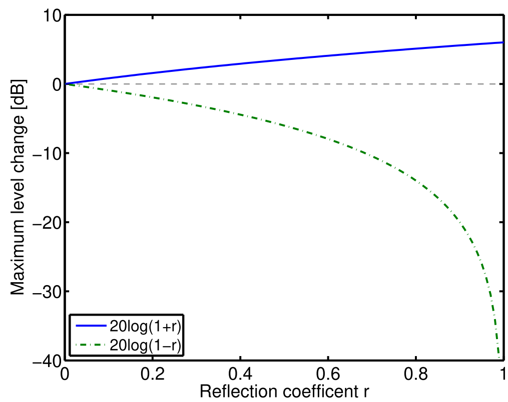

Fig. 12 Maximum amount of level variation assuming simple interference of the direct and reflected waves.

level variation.

4.5 Theoretical Analysis

4.5.1 Simplest Model

The distribution of momentary level shifts shown in Fig. 11 is asymmetric with respect to zero, but it is validated as described hereinafter. Ray tracing is a fundamental approach to model the propagation of electromagnetic waves [17]. Roughly speaking, a fuselage has the shape of cylinder. Therefore, the reflection is expected to radiate in all directions but the direction of the shadowed area. The theoretical maximum level variation is shown in Fig. 12, assuming a simple interference of the direct and reflected waves. It becomes

$$\Delta_x(n) = \begin{cases} 20\log(1+r) & \text{if in-phase} \\ 20\log(1-r) & \text{if anti-phase} \end{cases}, \tag{9}$$

where $\{r \in \mathbb{R} \mid 0 \le r \le 1\}$ is the reflection coefficient. From comparison of Figs. 11 and 12, it is reasonable to infer that the level variation is always less than 6 dB. Only when the total reflection is assumed does the amount of increase become 6 dB. However, because the minimum level variation could be minus infinity in this case, it leads to this asymmetry distribution with respect to zero.

4.5.2 Computer Simulation with Practical Parameters

Considering a practical topological relation between the direct path of BS signal and a reflection path by a flying airplane shown in Fig. 13, we estimate possible level variation through computer simulations. The settings of the computer simulations are presented in Table 3. Those are based on the actual parameter values for BS-1 channel [18]–[20].

In addition, we consider antenna gain variation depending on the incident angle of the BS radio frequency signal. The half-power beam width W of an aperture is generally calculated, in units of degrees, as

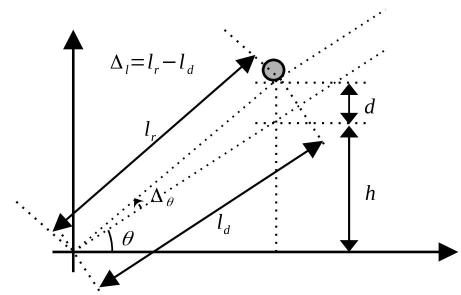

Fig. 13 Path length difference between a direct BS signal and one reflected by a flying object.

Table 3 Settings of computer simulation assuming a BS-1 channel.

Notation	Parameter	Value
c	speed of light	$3 \cdot 10^8$ m/s
f_s	sampling frequency	50.0 GHz
f_c	carrier frequency	11.72748 GHz
f_b	baud rate	28.86 Mbaud
B	signal band width	34.5 MHz
	modulation	8-PSK

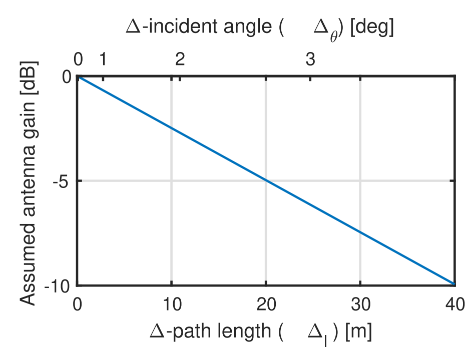

Fig. 14 Assumed antenna gain $\gamma(\Delta_l)$ as a function of path length difference Δ_l (bottom axis) and its corresponding incident angle of reflection wave Δ_θ (top axis).

$$W = \frac{k\lambda}{D}, \tag{10}$$

where D represents the antenna diameter, and λ denotes the wavelength of the signal. Also, k is a constant determined by the amplitude taper across the aperture [21]. For a typical parabolic antenna, $k = 70$ in degrees [22]. According to the datasheet of the BS antenna used in our measurement, $D = 0.45$. With $\lambda = c/f_c \simeq 0.0256$, we can obtain the half-power beam width of this antenna as approximately $W = 3.98$. For convenience, we assumed an antenna gain decaying linearly as the path length difference increases, as shown in Fig. 14. According to Figs. 14 and 15, this half-power point corresponds approximately to 750 m of the altitude difference from the direct path, which corresponds consecutively to 10 m of the path length difference, according to the same figure. Therefore, the received signal $y(n)$ is represented as

$$y(n) = s(n) + r\gamma(\Delta_l)s(n - \Delta_l/c), \tag{11}$$

where $\Delta_l = kc/f_s$ and $\gamma(\Delta_l)$ can be derived using the func-

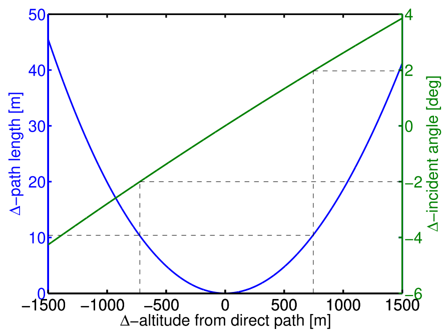

Fig. 15 Path length difference Δ_l (left axis) and its corresponding incident angle difference (right axis) as a function of the altitude difference from the direct path.

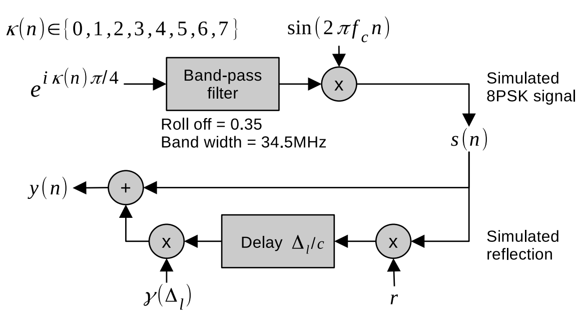

Fig. 16 8PSK signal generation and its propagation model assumed in computer simulations.

tion shown in Fig. 14.

Based on the topological relation shown in Fig. 13, the path length difference is definable as

$$\Delta_l = l_r - l_d \tag{12}$$

where

$$l_r = \sqrt{(h/\tan\theta)^2 + (h+d)^2}$$
$$l_d = h/\sin\theta + d\sin\theta.$$

Also,

$$\Delta_\theta = \arcsin\left(\frac{h+d}{l_r}\right) - \theta. \tag{13}$$

Figure 15 shows the path length difference represented by (12) and the incident angle difference represented by (13) as a function of d, assuming $\theta = 35.3°$, which is the elevation of BS satellite at the observation point in the experiment, and $(h + d) = 10{,}000$ m, which is approximately the altitude of tropopause. Additionally, the angle difference is superimposed in this figure on the right axis.

An 8PSK signal is generated as shown in Fig. 16. Symbol $\kappa(n)$ randomly takes an integer from 0 to 7 and changes its value at the symbol baud rate f_b. Parameters of the band-pass filter were set to the actual ones. After processing with the band-pass filter, it is upconverted with the carrier signal to generate a simulated 8PSK signal $s(n)$. The mixing process along propagation is depicted as the lower part of this figure. The reflection wave is made from the 8PSK signal by being multiplied by a reflection coefficient r, delayed with Δ_l/c and then further multiplied by the antenna gain $\gamma(\Delta_l)$. This reflection wave is added directly to the direct wave $s(n)$ to simulate the received signal $y(n)$, ignoring the effects of circular polarization. Therefore, the possible level change Δ_x in the received BS signal is calculated using

$$\Delta_x = 10\log_{10}\left(\sum_n |y(n)|^2\right) - 10\log_{10}\left(\sum_n |s(n)|^2\right). \tag{14}$$

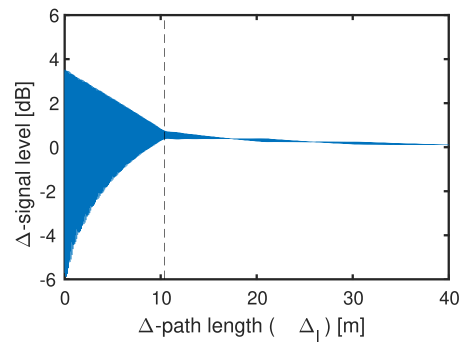

Fig. 17 Simulated level change Δ_x with $r = 0.5$ assuming 8PSK as a function of path length difference Δ_l. The dashed line shows the path length difference corresponding to the period of the symbol baud rate of the BS signal.

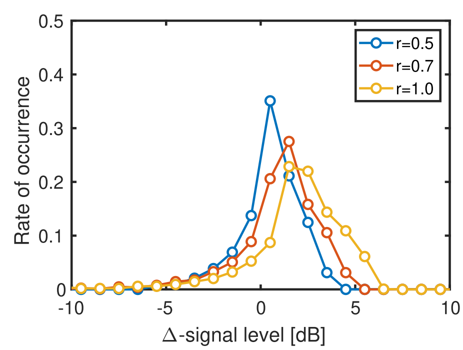

Fig. 18 Histogram of the simulated level changes for $0 \leq \Delta_l < c/f_b$ shown in Fig. 17

Figure 17 depicts (14) as a function of path length difference Δ_l, which affects $y(n)$ in (14).

Figure 15 suggests that the path length difference is approximately 20 m, even when the altitude of the flying airplane is 1 km above or below the direct path of the BS signal ($d = \pm 1{,}000$ in Fig. 13). For comparison with the results shown in Fig. 11, the histogram of Fig. 17 is calculated using data within $0 \leq \Delta_l < c/f_b$. This upper limit was chosen as the path length difference corresponding to the period of the symbol baud rate. Figure 18 portrays the result. It asymptotically resembles Fig. 11 with respect to its range and shape.

Considering the baud rate of the actual BS signal shown in Table 3, it is reasonable to infer that the signal level difference occurs when the arrival time difference between the direct and reflected waves is less than approximately $1/0.02886 = 34.65$ ns because, under this condition, the same symbol certainly overlaps in some part. This arrival time difference corresponds to 10.4 m of the path length difference. According to Fig. 13, this condition is satisfied when an airplane is flying within 750 m above or below the direct propagation path of the BS radio wave. This situation is more likely than for the case in which an airplane is flying within the first Fresnel zone discussed in Sect. 3.1.

5. Discussion

It is speculated through careful analysis that a promising cause of the momentary level shifts is an aircraft flying overhead. To support this assumption further, the level of receiving BS signal is shown together with lines indicating the timing by which flights bound for Tokyo from Sapporo are expected to pass by the propagation path of the BS radio frequency signal received in Sendai. Figure 19 presents the result. As might be apparent in this figure, the appearance of momentary level shifts generally coincides with the timing of airplanes passing overhead. This fact supports and concurs with the assumption that the cause of the momentary level shifts is an airplane. We infer that the noise appearing at Kashima during 10:00 to 12:00 could be attributed to scattering by cloud or water vapor in the atmosphere because it is not momentary and has some duration.

If an object is cylindrical, then it is expected that an electromagnetic wave is reflected toward various directions, depending on the incident angle. In this case, interference occurs irrespective of the observation point. The location of Kashima is approximately 30 km northeast from Narita International Airport, from which flights frequently depart and to which flights arrive throughout the day. Nevertheless, the data observed in Kashima include no such level shift. This lack of level shift can be attributed to the directivity pattern of a parabolic antenna. Because the airport is sufficiently close, airplanes are flying far lower than the propagation path of BS radio waves. When the reflected waves are coming largely from off-axis, the received signal level would be too weak to interfere with the direct wave, resulting in no appearance of momentary level shift.

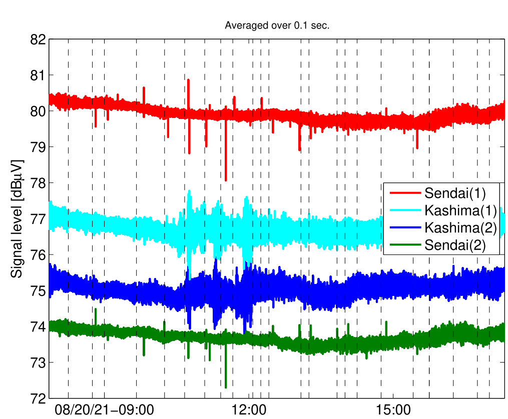

Fig. 19 Example of the observed BS signal level superimposed with the timing of flights passing overhead (dashed lines).

As shown in Fig. 2, CS radio waves are mapped onto IF signals of different frequencies from BS radio waves. Therefore, observing IF signals of not only BS signals but also CS ones would consolidate the conclusion of this paper if momemtary level shifts appear in both IF signals becauase they have different sources.

6. Conclusion

Routine observation of the level of BS signals revealed that momentary level shifts can be present multiple times, especially during the daytime. Findings from thorough statistical investigation of the level shifts strongly suggest the cause of the level shifts as aircraft flying approximately at the altitude of the tropopause. The results also suggest that, in many cases, these level shifts are attributed to reflection by an airplane rather than its shadowing. Moreover, results indicate that an airplane within a range of approximately 1,500 m height might affect the signal level. Therefore, careful attention must be used when one applies the level of BS signal for use with remote sensing. Moreover, results show that observation of the BS signal might be used similarly to a bistatic radar to monitor an object that is flying in the sky. Future works will include optimization of parameters α and T for improving the detection rate without an increase in the false positive rate.

Acknowledgments

We thank Dr. Murata and Prof. Suzuki for their valuable comments related to this study.

References

[1] S. Yokozawa, M. Kamei, and H. Sujikai, "Rain attenuation characteristics for 21-Ghz-band satellite broadcasting measured by beacon signal," 2019 International Symposium on Antennas and Propagation (ISAP), pp.1–3, 2019.
[2] C.M. Rush, F.G. Stewart, M. PoKempner, and R. Reasoner, "Some ionospheric factors affecting the coverage of an HF/VHF direct broadcasting satellite service," IEEE Trans. Antennas Propag, vol.34, no.4, pp.475–482, 1986.
[3] T. Kan, B. Jeong, H. Susukita, K. Kawasaki, T. Takahashi, and M. Toyoshima, "Experimental results of seasonal variation of shadowing by Ka-band mobile satellite communication," Trans. Japan Society for Aeronautical and Space Sciences, Aerospace Technology Japan, vol.18, no.6, pp.363–368, Nov. 2020.
[4] Y. Karasawa and T. Matsudo, "One-minute rain rate distributions in Japan derived from AMEDAS one-hour rain rate data," IEEE Trans. Geosci. Remote Sens., vol.29, no.6, pp.890–898, Nov. 1991.
[5] R. Nishimura, B. Jeong, K. Kawasaki, and T. Takahashi, "An attempt of rainfall estimation by monitoring broadcasting satellite combined with machine learning," IEICE Technical Report, vol.118, no.442, pp.123–128, Feb. 2019 (in Japanese).
[6] S. Kawamura, H. Ohta, H. Hanado, M.K. Yamamoto, N. Shiga, K. Kido, S. Yasuda, T. Goto, R. Ichikawa, J. Amagai, K. Imamura, M. Fujieda, H. Iwai, S. Sugitani, and T. Iguchi, "Water vapor estimation using digital terrestrial broadcasting waves," Radio Sci., vol.52,

no.3, pp.367–377, March 2017.
[7] M. Nagahora, M. Takahashi, Y. Morita, and H. Sakurada, “Receiving field strength fluctuation by aircraft scattering,” ITE Technical Report, vol.22, no.11, pp.43–48, Feb. 1998 (in Japanese).
[8] J.I. Glaser, “Bistatic RCS of complex objects near forward scatter,” IEEE Trans. Aerosp Electron. Syst., vol.21, no.1, pp.70–78, Jan. 1985.
[9] R.C. MacCamy, “On Babinet’s principle,” Canadian Journal of Mathematics, vol.10, pp.632–640, 1958.
[10] R. Nishimura, B. Jeong, H. Susukita, and T. Takahashi, “A potential cause of pulsive noises in receiving BS signals,” IEICE Technical Report, vol.121, no.189, pp.17–22, Oct. 2021.
[11] https://www.soumu.go.jp/main_content/000730686.pdf (in Japanese), accessed July 5. 2022.
[12] A. Osterman and P. Ritosa, “Radio propagation calculation: A technique using 3D Fresnel zones for decimeter radio waves on LIDAR data,” IEEE Antennas Propag. Mag., vol.61, no.6, pp.31–43, 2019.
[13] https://www.ana.co.jp/ja/jp/domestic/departure/inflight/seatmap/detail/b6h.html (in Japanese), accessed April 25. 2022.
[14] L.A. Hajkowicz, “Possible ambiguity in defining the ionospheric origin of quasiperiodic scintillations,” Journal of Atmospheric and Solar–Terrestrial Physics, vol.59, no.12, pp.1417–1423, Aug. 1997.
[15] “Flight schedule on new Chitose Airport terminal,” https://www.new-chitose-airport.jp/ja/airport/time/result/?ap=dom&type=dep&po=HND&co=&tf=4&tt=26&f=, accessed Aug. 19. 2021.
[16] “Flightradar24: Live flight tracker,” https://www.flightradar24.com, accessed Aug. 13. 2021.
[17] Z. Yun and M.F. Iskander, “Ray tracing for radio propagation modeling: Principles and applications,” IEEE Access, vol.3, pp.1089–1100, 2015.
[18] K. Saito, “Operational guidelines for ISDB-S3,” ITE Technical Report, vol.40, no.45, pp.47–52, Dec. 2016.
[19] ARIB STD-B44 Version 2.1, “Transmission system for advanced wide band digital satellite broadcasting (ISDB-S3),” standard, Association of Radio Industries and Businesses, 2016.
[20] The Radio Use Web Site, “Frequency assignment plan (as of November 2021),” Technical Report, Japanese Ministry of Internal Affairs and Communications, Nov. 2021. Annex 1-2.
[21] K.L. Walton and V.C. Sundberg, “Constant-beamwidth antenna development,” IEEE Trans. Antennas Propag., vol.16, no.5, pp.510–513, 1968.
[22] D. Minoli, Satellite Systems Engineering in an IPv6 Environment, CRC Press, 2019.

Ryouichi Nishimura was conferred a B.S. degree in Information Engineering in 1993 and M.Sc. and Ph.D. degrees in Information Science in 1995 and 1998, respectively, all from Tohoku University, Sendai Japan. During 1998 2000, he was a Visiting Researcher at ATR, Media Information and Communications Research Laboratories, Kyoto, Japan. He was a Research Associate at Tohoku University during 2000 2004, and then an Associate Professor until November 2006. He is currently a Research Expert at the National Institute of Information and Communications Technology (NICT), Sendai Japan, where he has been working mostly on audio signal processing and remote sensing for disaster management.

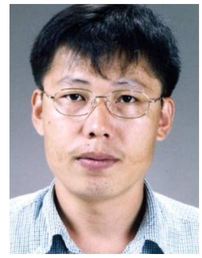

Byeongpyo Jeong After completing a doctoral course, he worked for National Research Institute of Fire and Disaster, and joined in NICT in 2012. He is engaged in research on disaster response application using satellite communication. Ph.D. (Engineering).

Hajime Susukita obtained a Master of Engineering degree at Akita University, Akita Japan in 1997. After working mainly as a field engineer, he is currently a technical researcher at the National Institute of Information and Communications Technology (NICT), Sendai Japan, engaged to support technical works focusing on the wireless communication technology.

Takashi Takahashi received the B.E. and M.E. degrees in electronics engineering from University of Electro-Communications, Tokyo, Japan, in 1989 and 1991, respectively. He joined the National Institute of Information and Communications Technology (NICT: former CRL) in 1991, and he has been engaged in experimental research on mobile and fixed satellite communication systems. During 2002–2005, he joined the Japan Aerospace Exploration Agency (JAXA: former NASDA). He is now an Associate Director of Space Communication Systems Laboratory, NICT. He works in ETS-9 project (Engineering Test Satellite No.9).

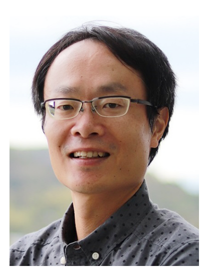

Kenichi Takizawa received the B.E., M.E., and Ph.D. degrees in engineering from Niigata University, in 1998, 2000, and 2003, respectively. He joined the National Institute of Information and Communications Technology, in 2003. From 2011 to 2012, he stayed with Aalto University, Finland, as a Visiting Researcher. He received the Young Researcher’s Award from IEICE, in 2006. (Member, IEEE)